

PLANNING OF MEASUREMENT SERIES FOR THERMODYNAMIC PROPERTIES BASED ON OPTIMAL EXPERIMENTAL DESIGN

Ophelia Frotscher*

Roland Herzog[†]

Markus Richter*

Decreasing the time required for accurate thermodynamic property measurements is extremely desirable for model development, that can respond to the needs of science and industry within a short time frame. Here, we demonstrate the application of optimal experimental design to measurements of thermodynamic properties. The technique is exemplified using the fitting of a Schilling-type equation from published (p, ρ, T) -measurements of ethylene glycol and propylene glycol. The analysis shows that a fixed-exponent fit using (p, T) -measurements along the five most informative isotherms produces models of relative density errors comparable to those obtained using the data along all isotherms. It is also argued that a calculation of optimal isotherms prior to the measurement series can further increase the precision at no additional experimental effort.

Keywords. optimal experimental design, correlation, density, ethylene glycol, measurement

1 INTRODUCTION

For scientific but particularly for industrial applications, it is absolutely valuable to provide equations of state (EOS) that accurately describe the thermodynamic behavior of the concerned fluid substances within a narrow time frame. However, accurate thermodynamic models are usually based on reliable experimental data, thus, the development can require quite a long time since accurate measurements over wide temperature and pressure ranges are typically a time-consuming endeavor. Here, we demonstrate the advantages of involving optimal experimental design (OED) in the process of planning measurement series for thermodynamic properties with the goal to deliberately reduce the experimental effort, thus, decreasing the overall time for model development. Therefore, the issue with typical

*Technische Universität Chemnitz, Faculty of Mechanical Engineering, Professorship Applied Thermodynamics, 09107 Chemnitz, Germany (ophelia.frotscher@mb.tu-chemnitz.de, <https://www.tu-chemnitz.de/mb/TechnThDyn/personal.php>, ORCID 0000-0002-6915-1988, m.richter@mb.tu-chemnitz.de, <https://www.tu-chemnitz.de/mb/TechnThDyn/personal.php>, ORCID 0000-0001-8120-5646).

[†]Technische Universität Chemnitz, Faculty of Mathematics, Professorship Numerical Mathematics (Partial Differential Equations), 09107 Chemnitz, Germany (roland.herzog@mathematik.tu-chemnitz.de, https://www.tu-chemnitz.de/mathematik/part_dgl/people/herzog, ORCID 0000-0003-2164-6575).

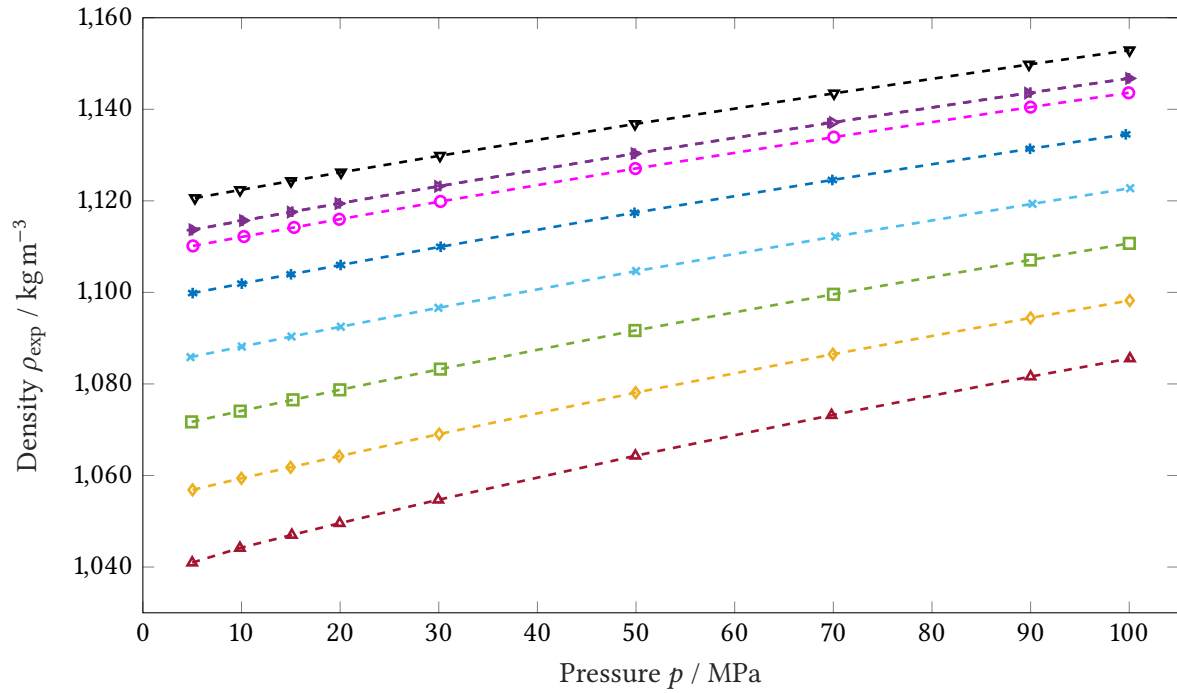


Figure 1.1: Experimental densities (symbols) and interpolated densities (dashed lines) measured by Yang et al. [Yang et al., 2020](#). ∇ , $T \approx 283.32$ K; $+$, $T \approx 293.14$ K; \triangleright , $T \approx 293.14$ K; \circ , $T \approx 298.18$ K; $*$, $T \approx 313.13$ K; \times , $T \approx 333.09$ K; \square , $T \approx 353.13$ K; \diamond , $T \approx 373.22$ K; \triangle , $T \approx 393.09$ K

experimental design and the approach of OED will be explained using our density data of ethylene glycol published by Yang et al. [Yang et al., 2020](#) and the density data of propylene glycol measured with the same instrument published by Sampson et al. [Sampson et al., 2019](#). The application of OED is described using the measurements for ethylene glycol, which are shown in [Fig. 1.1](#). The (p, ρ, T) behavior of ethylene glycol was investigated over the temperature range from $T = (283.3 \text{ to } 393.1)$ K at pressures from $p = (4.8 \text{ to } 100.1)$ MPa utilizing a high-pressure vibrating-tube densimeter; a total of 89 (p, ρ, T) data points were studied with a combined expanded uncertainty ($k = 2$) of 1.57 kg m^{-3} (equivalent to a max. relative uncertainty of 0.151 %). To model the experimental data, in Yang et al. [Yang et al., 2020](#) two empirical Schilling-type correlation equations were fitted [Schilling, Kleinrahm, Wagner, 2008](#): one of the same form (same number of terms, same exponents) as for propylene glycol in the work of Sampson et al. [Sampson et al., 2019](#) (fixed exponent model), and one using the "artificial intelligence powered" software tool Eureqa (Eureqa model) [Schmidt, Lipson, 2009; 2015](#). The first approach results from the assumed thermodynamic similarity of both substances, and the second approach serves to investigate the applicability of symbolic regression and machine learning for the optimization of correlation equations. [Section 2](#) of the present paper provides a small overview of different types of correlation models for liquid-phase densities to support the understanding of the choices made in this work.

In the present study, we illustrate how OED could have been used for the planning of the measurement series conducted by Yang et al. [Yang et al., 2020](#) in order to reduce the amount of density measurements of ethylene glycol needed to reliably adjust the parameters of the fixed exponents model. To validate our results regarding the benefits of OED, the calculations were also applied to measured densities

of propylene glycol [Sampson et al., 2019](#). In spite of its capabilities to select measurements with the highest information content, OED is hardly applied in the field of thermodynamic property research. We conjecture that the primary reasons for this are:

- a lack of knowledge about OED technologies,
- the lack of software tools for easy application of OED,
- the requirement to specify the underlying model beforehand.

For a detailed overview of the use of OED in different areas of chemical and thermal engineering research, we refer the reader to Francheschini and Macchietto [Francheschini, Macchietto, 2008](#). With respect to thermodynamic property research, we point out the work of Bardow and colleagues [Rasch, Bucker, Bardow, 2009](#); [Dechambre et al., 2014](#), which deals with the experimental characterization of liquid-liquid equilibria utilizing OED. In contrast to those investigations, the present work focuses on the temperature and pressure values for density measurements, with the aim to minimize the parameter variance of the correlation model. The method described here can be used equivalently for measurements of other thermodynamic and transport properties (e. g., speed of sound, specific heat capacity, viscosity, etc.).

When changing the isotherm in a usual measurement series, establishing thermal equilibrium with a typical (p, ρ, T) apparatus is rather time-consuming compared to setting new pressures along an isotherm. For this reason, we decided to use OED to select a subset of the most informative isotherms. OED can be imagined as an in-situ tool within the following workflow:

- (a) choose an initial set of (p, T) state points to be studied (e. g., two isotherms à five pressures),
- (b) conduct the measurements (e. g., density),
- (c) fit the model (e. g., the Schilling-type model),
- (d) answer the following questions:
 - Can the model reproduce the measured data with sufficient accuracy (e. g., within the experimental uncertainty)?
 - Can a significant amount of information be gained from additional measurements?
- (e) If the latter is not the case, the experiment is terminated. Otherwise, select the next most relevant isotherm using OED ([Section 3](#)) and proceed with [item \(b\)](#).

In this paper, we utilize OED to select a subset of isothermal experiments from a two given sets of measurements, which are already available. We use the measurements selected to fit the parameters for new fixed and free exponent models for ethylene glycol and propylene glycol. The results are compared to the existing models ([Section 4](#)).

2 MODELING APPROACH

For simulations in process engineering, accurate and easily applicable models that describe the real fluid behavior are needed. Considering the lack of knowledge about more complex compounds at the molecular level, empirical equations of state have become an established way of modeling thermodynamic behavior. In industrial applications, the empirical Tait equation (1888) is still widely used to model densities of liquids [Gibson, Loeffler, 1939](#). However, a contemporary approach to model liquid-phase densities was developed by Schilling et al. [Schilling, Kleinrahm, Wagner, 2008](#). This is an equation in form of polynomial terms, which is based on the relationship to fundamental equations of state.

For the modeling of fundamental equations of state, which provide the possibility to derive all thermodynamic properties by differentiation of these equations, functional forms such as polynomial and exponential terms are involved [Span, 2000](#); [Thol, Bell, 2020](#). In the past, within the scope of developing fundamental equations, Setzmann and Wagner (1989) [Setzmann, Wagner, 1989](#); [Span, 2000](#) established the modeling tool OPTIM, which combines a modified step-wise regression analysis based on a “*bank of terms*” with elements of evolutionary optimization methods. Nowadays, this tool is mostly unused. However, it was applied to model the density of liquid *n*-heptane, *n*-nonane, 2,4-dichlorotoluene and bromobenzene in the temperature range from 233.15 to 473.15 K at pressures up to 30 MPa by Schilling et al. [Schilling, Kleinrahm, Wagner, 2008](#). Due to its good representation of liquid-phase experimental data, further works, e. g., of Sommer et al. [Sommer et al., 2011](#), Sampson et al. [Sampson et al., 2019](#) (Table 4.3, propylene glycol - fix Exp.) and Yang et al. [Yang et al., 2020](#) (Table 4.3, ethylene glycol - fix Exp.), also relate to this equation. The so-called Schilling-type equation has the following functional form:

$$\frac{\rho}{\rho_0} = \sum_{j=1}^{I_{\text{Pol}}} n_j \sigma^{t_j} \pi^{p_j} \quad (2.1)$$

$$\sigma = (T/T_0 - 1) \text{ and } \pi = (p/p_0 + 1) \quad (2.2)$$

The parameters σ and π represent the reduced temperature and the reduced pressure, respectively, while T_0 , p_0 and ρ_0 are chosen by the measured values and I_{Pol} defines the number of terms. In Sampson et al. [Sampson et al., 2019](#), the parameters were set to $T_0 = 150$ K, $p_0 = 100$ MPa and $\rho_0 = 1000$ kg m⁻³, and n_j , t_j and p_j were fitted to the experimental data of propylene glycol setting the number of terms $I_{\text{Pol}} = 8$. With this model, the measured densities for propylene glycol can be reproduced within a maximum error of $\varepsilon_R = 0.015$ %. Due to the similarity between both substances, the same setup was used to fit the parameters n_j for ethylene glycol in Yang et al. [Yang et al., 2020](#), keeping the exponents t_j and p_j fixed (fixed exponent model, Table 4.3). The experimental data of ethylene glycol is represented within a maximum error of $\varepsilon_R = 0.025$ %.

Most current modeling approaches, especially for non-linear models, have a high development effort and the requirement of thorough background knowledge in common. In the work of Yang et al. also a new approach utilizing Eureqa was employed to investigate the suitability of a machine learning tool for non-linear EOS modeling [Schmidt, Lipson, 2009](#); [2015](#). The form of terms was chosen equivalent to the existing model, while the aim was to reduce the number of terms, to fit the exponents and to stay within an adequate uncertainty (Eureqa model, Table 4.3). In addition to the less complex functional form, a maximum error of $\varepsilon_R = 0.020$ % and a better extrapolation behavior are achieved. Table 2.1 gives an overview of the different modeling approaches.

Table 2.1: Features of different EOS modeling approaches for liquid-phase densities (Tait equation [Gibson, Loeffler, 1939](#), Schilling-type equation [Schilling, Kleinrahm, Wagner, 2008](#), Eureka modeling [Schmidt, Lipson, 2009; 2015](#))

EOS type	Feature
Tait	well-established model, widely used for liquid densities predefined model form requires custom fitting algorithm
Schilling	simple model form, related to fundamental EOS user-specific number of terms requires custom fitting algorithm
Eureka	intuitive software handling symbolic regression based on genetic algorithms comparing complexity and uncertainty

3 BACKGROUND ON OPTIMAL EXPERIMENTAL DESIGN

Optimal experimental design is a technique to select experiments which are most informative about the unknown parameters of a given model. We refer the interested reader to Pázman, Uciński and Atkinson et al. [Pázman, 1986](#); [Uciński, 2005](#); [Atkinson, Donev, Tobias, 2007](#) for a comprehensive background. Here, we use OED to reduce the experimental effort required to identify the parameters n_j , $j = 1, \dots, I_{\text{Pol}}$, in (2.1) with exponents t_j and p_j fixed. In this case, the dependent variable ρ/ρ_0 is a linear function of the parameters, which simplifies the subsequent description. To be specific, we deduce from (2.1) that each triple of measured data (p_i, ρ_i, T_i) , after conversion to reduced quantities $(\pi_i, \rho_i/\rho_0, \sigma_i)$, contributes a prediction of the form $\rho_i \approx \rho_0 j(\pi_i, \sigma_i) n$, where $n = (n_1, \dots, n_8)^T \in \mathbb{R}^8$ denotes the parameter vector and

$$j(\pi_i, \sigma_i) = [\sigma_i^{t_1} \pi_i^{p_1} \quad \dots \quad \sigma_i^{t_8} \pi_i^{p_8}] \quad (3.1)$$

is the so-called elementary Jacobian associated with the i -th measurement. Following the theory of OED, the information content of a single measurement is expressed through the elementary Fisher information matrix (FIM) $I_i = j(\pi_i, \sigma_i)^T j(\pi_i, \sigma_i) \in \mathbb{R}^{8 \times 8}$. Each elementary FIM is a symmetric, positive semi-definite rank-1 matrix. Moreover, since we can assume individual measurements to be statistically independent, the FIM associated with a series of experiments is obtained as $I = \sum_i I_i$.

It is common to apply a scalar objective function, which converts the FIM associated with any collection of experiments into a single number and, thus, allows a comparison with any other collection of experiments. We utilize here the A-criterion

$$\Psi_A(I) = \text{trace}(I^{-1}) = \sum_{j=1}^8 \frac{1}{\lambda_j}, \quad (3.2)$$

where λ_j is the j -th eigenvalue of I . Clearly, at least eight individual measurements are required to render the FIM positive definite and the criterion $\Psi_A(I)$ finite. In this case, the value of $\Psi_A(I)$ is proportional to the sum of the squared semi-axes of confidence ellipsoids in the 8-dimensional

parameter space. Consequently, we seek to minimize $\Psi_A(I)$, possibly subject to constraints on the experimental budget, in order to maximize the information content of the collection of experiments selected and simultaneously minimize parameter variation in the face of measurement errors.

As we argued in the introduction, it is advantageous from a practical point of view to take measurements along an isotherm. In the following section, we will therefore optimize over experiments each of which comprises several measurements obtained by varying the pressure along an isotherm.

4 NUMERICAL RESULTS

The approach described in [Section 3](#) is used to optimize the measurement series by maximizing the information contained in a set of eight isothermal measurements at approximate temperatures $T = (283, 293, 298, 313, 333, 353, 373 \text{ and } 393) \text{ K}$ drawn from the experiments conducted by Yang et al. [Yang et al., 2020](#). The measurement plan for each isotherm consists of nine pressure values, approximately $p = (5, 10, 15, 20, 30, 50, 70, 90 \text{ and } 100) \text{ MPa}$. [Fig. 4.1 a\)](#) and [Table 4.1](#) show the most informative selection of isotherms (black dots) to fit the parameters n_1, \dots, n_8 using a varying number of isotherms. As expected, the value of the objective [\(3.2\)](#) decreases as we allow more isotherms to be included. However, when transitioning from five to six isotherms, the further decrease in the objective is small compared to the previous steps. For propylene glycol, measured at approximate temperatures $T = (273, 283, 293, 298, 313, 333, 353, 373 \text{ and } 393) \text{ K}$, [Fig. 4.1 b\)](#) and [Table 4.2](#) show a similar selection of best isotherms and for the decay of the objective function values. In this case, the measurement plan for each isotherm consists of eight pressure values, approximately $p = (5, 10, 15, 20, 30.5, 50.5, 71 \text{ and } 91) \text{ MPa}$.

We aim to compare the accuracies of the fixed exponent model [\(2.1\)](#) for ethylene glycol, once with parameters n_1, \dots, n_8 fitted from the complete set of experiments and once using only the five best isotherms ([Table 4.3 fixE-5](#)). To this end, we show in [Fig. 4.2 a\)](#) and [c\)](#) the relative deviations of calculated densities from experimental values as a function of pressure along all eight isotherms. It can be seen that using only five out of eight isotherms for the fitting process yields a greatest deviation only larger by approximately 0.003 %. The same approach is used to fit a new model for propylene glycol to the best five isotherms, see the lower part of [Table 4.3 \(fixE-5\)](#). With an absolute difference in the greatest deviation of 0.0015 % for propylene glycol between the two fixed exponent models ([Fig. 4.3 a\)](#) and [b\)](#)), the result for OED is even more promising than for ethylene glycol.

Next, we investigate the information gain obtained by allowing the temperatures of the isothermal experiments to be chosen freely within the interval from $T = 283 \text{ K}$ to $T = 393 \text{ K}$ for ethylene glycol and $T = 273 \text{ K}$ to $T = 393 \text{ K}$ for propylene glycol. To this end, we introduce an equidistant grid of possible temperature values with a spacing of 2 K, and pressure values for each group of isothermal experiments are the same as measured. The optimal selections of up to five isotherms can be found in [Fig. 4.1 a\)](#) and the bottom half of [Table 4.1](#) for ethylene glycol as well as in [Fig. 4.1 b\)](#) and the bottom half of [Table 4.2](#) for propylene glycol.

By comparing both selection approaches, the similarity of temperatures for the best two and three isotherms as well as the difference between those for the four and five best isotherms are noticeable.

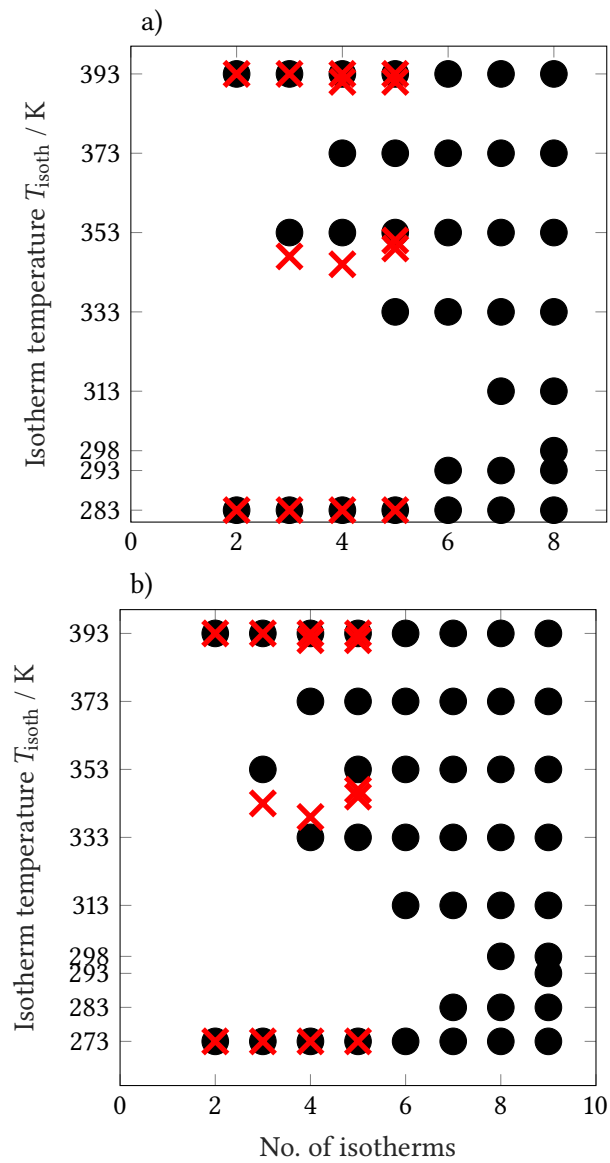


Figure 4.1: Selection of the best isotherms • from the measured isotherms and x from a free choice a) for ethylene glycol between $T = (283 \text{ to } 393) \text{ K}$ and b) for propylene glycol between $T = (273 \text{ to } 393) \text{ K}$, within a raster of 2 K using the A-criterion (3.2) to minimize the parameter uncertainty

Table 4.1: Selection of the best isotherms for different numbers of isotherms and the objective value for ethylene glycol

No. of isotherms	measured isotherms best choice K	objective value
2	393.09 and 283.32	23 782.87
3	393.09, 283.32 and 353.13	120.32
4	393.09, 283.32, 353.13 and 373.22	94.40
5	393.09, 283.32, 353.13, 373.22 and 333.09	78.82
6	393.09, 283.32, 353.13, 373.22, 333.09 and 293.14	73.07
7	393.09, 283.32, 353.13, 373.22, 333.09, 293.14 and 313.13	68.36
8	393.09, 283.32, 353.13, 373.22, 333.09, 293.14, 313.13 and 298.18	65.77
No. of isotherms	free isotherms best choice K	objective value
2	283.00 and 393.00	23 113.13
3	283.00, 347.00 and 393.00	119.83
4	283.00, 345.00, 391.00 and 393.00	85.98
5	283.00, 349.00, 351.00, 391.00 and 393.00	69.22

This leads us to expect an improvement of the model with a fit to the free best five isotherms. However, due to the missing measured values, no comparable model can be developed for this case.

Instead, we investigate the importance of the functional form by fitting a new model to the best five measured isotherms, where also the exponents are optimized (Fig. 4.2 d) and Table 4.3 freeE-5). Here, even with five isotherms, the maximum deviations can be reduced significantly. However, for propylene glycol, the free exponent model shows large deviations for the isotherms not selected (greatest deviation 0.0431 %) compared to the deviation of the selected isotherms in the free exponent model (greatest deviation 0.0046 %) (Fig. 4.3 c)) and compared to the model published by Sampson et al [Sampson et al., 2019](#) (Table 4.3, propylene glycol - fix Exp.). This behavior in conjunction with the conclusion of Yang et al. [Yang et al., 2020](#) concerning the Eureka model (Fig. 4.2 b)), demonstrates the importance of a comprehensive model optimization. To exploit the potential of free exponent modeling, we plan to employ the sequential OED approach, described in Section 1, for calculating the necessary isotherms based on nonlinear models in future work.

For a more comprehensive model examination between the modeling approach by Eureka and by the typical Schilling-type fit, the extrapolation behavior was investigated taking the example of ethylene glycol. Therefore, the models were compared to an unpublished fundamental equation of state in form of the Helmholtz energy as implemented in REFPROP [Lemmon et al., 2018](#). This model is valid within the following limits:

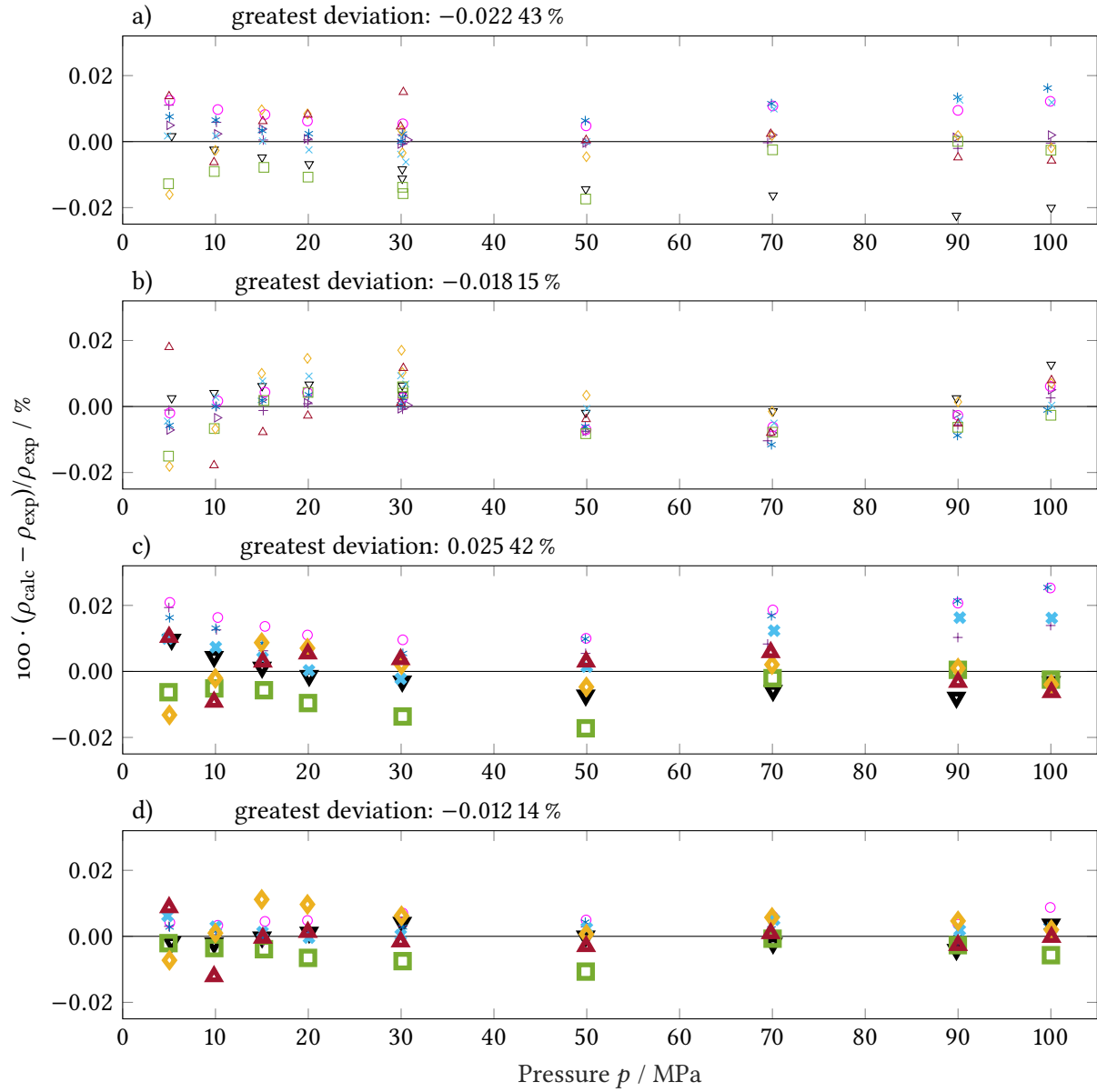


Figure 4.2: Relative deviations of **ethylene glycol** densities calculated with different models from experimental values, a) fixed exponent model fitted with all eight measured isotherms, b) Eureka model fitted with all eight measured isotherms, c) fixed exponent model fitted with the best five measured isotherms (bold marker), d) free exponent model fitted with the best five measured isotherms (bold marker). ∇ , $T \approx 283$ K; $+$, $T \approx 293$ K; \triangleright , $T \approx 293$ K; \circ , $T \approx 298$ K; $*$, $T \approx 313$ K; \times , $T \approx 333$ K; \square , $T \approx 353$ K; \diamond , $T \approx 373$ K; \triangle , $T \approx 393$ K

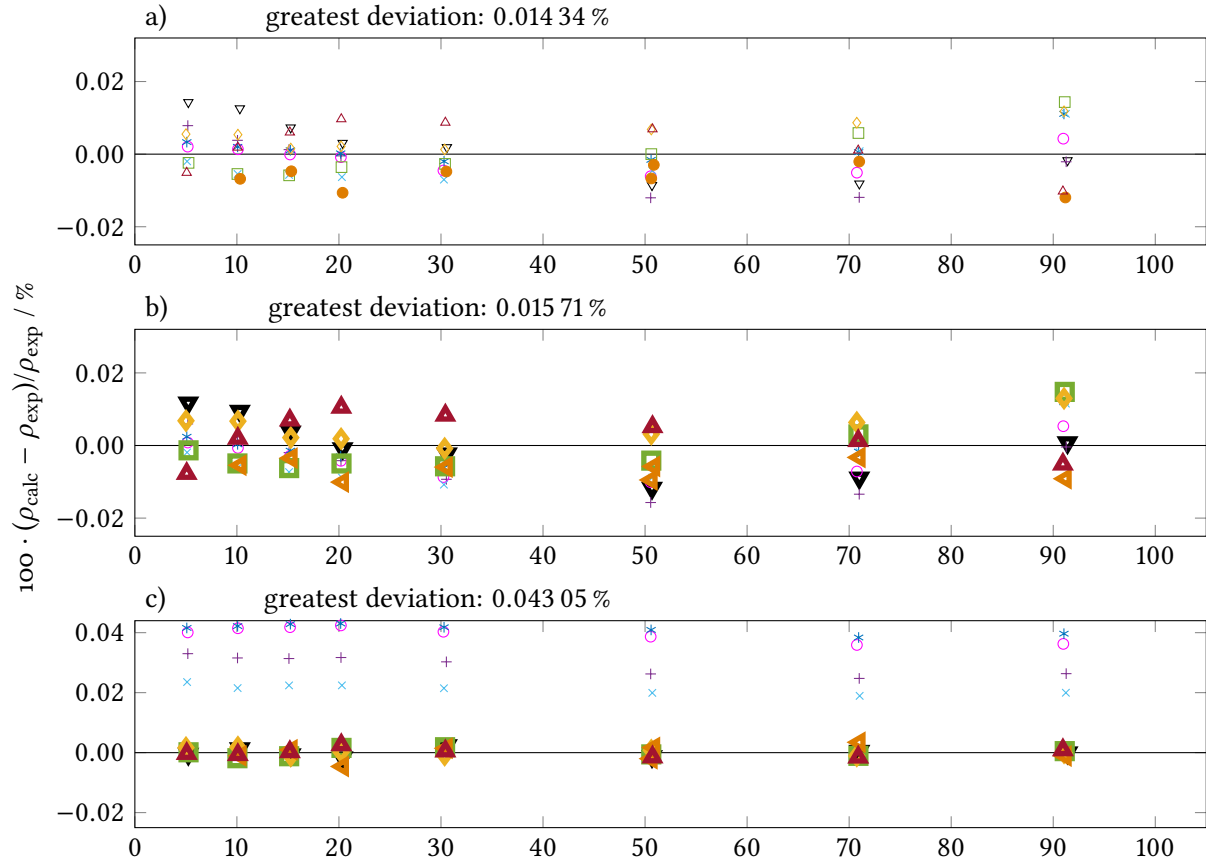


Figure 4.3: Relative deviations of **propylene glycol** densities calculated with different models from experimental values, a) fixed exponent model fitted with all nine measured isotherms, b) fixed exponent model fitted with the best five measured isotherms (bold marker), c) free exponent model fitted with the best five measured isotherms (bold marker). ∇ , $T \approx 273$ K; $+$, $T \approx 283$ K; \circ , $T \approx 293$ K; $*$, $T \approx 298$ K; \times , $T \approx 313$ K; \square , $T \approx 333$ K; \diamond , $T \approx 353$ K; \triangleleft , $T \approx 373$ K; \triangle , $T \approx 393$ K

Table 4.2: Selection of the best isotherms for different numbers of isotherms and the objective value for propylene glycol

No. of isotherms	measured isotherms best choice K	objective value
2	272.73 and 392.95	37 026.60
3	272.73, 392.95 and 352.99	145.84
4	272.73, 392.95, 373.34 and 333.05	107.35
5	272.73, 392.95, 352.99, 373.34 and 333.05	90.86
6	272.73, 392.95, 352.99, 373.34, 333.05 and 313.12	83.26
7	272.73, 392.95, 352.99, 373.34, 333.05, 313.12 and 283.18	78.56
8	272.73, 392.95, 352.99, 373.34, 333.05, 313.12, 283.18 and 298.12	75.55
9	272.73, 392.95, 352.99, 373.34, 333.05, 313.12, 283.18, 298.12 and 293.18	73.47
No. of isotherms	free isotherms best choice K	objective value
2	273.00 and 393.00	35 604.70
3	273.00, 343.00 and 393.00	144.11
4	273.00, 339.00, 391.00 and 393.00	98.78
5	273.00, 345.00, 347.00, 391.00 and 393.00	80.83

- temperature: $T = 260.6$ to 750.0 K,
- pressure: up to $p = 100$ MPa,
- density: up to $\rho = 1136.5$ kg m⁻³,
- vapor-liquid saturation line.

The vapor-liquid saturation line defines the limit for extrapolation up to the maximum temperature and the minimum pressure. To calculate the liquid densities with the different models at the saturation line, the corresponding temperatures and pressures from REFPROP (Fig. 4.4) are used. As already shown in the paper from Yang et al. Yang et al., 2020, the Eureka model (Fig. 4.4) shows the best extrapolation behavior within ± 2 % up to $p = 4.5$ MPa and $T = 655$ K with $\rho \approx 740$ kg m⁻³. The graphs for the fixed exponent model and the fixed exponent model with the best five measured isotherms in Fig. 4.4 are similar, while the free exponent model fitted to the best five measured isotherms shows the largest deviations from the densities calculated with the fundamental equation in REFPROP. It is important to note that none of the models reproduces the curvature of densities calculated from the fundamental equation in REFPROP, which means that they are all strictly limited to the calculation of liquid-phase densities.

Many applications work at pressures below 5 MPa. For this reason, we have extrapolated the measured isotherms to ambient pressure. All models reproduce the values within relative deviations of -0.28 to -0.1 %. Each model shows the largest deviation at the 393 K isotherm, and again, the Eureka model

Table 4.3: Coefficients of (2.1) for the fixed exponent model (fix. Exp.), the Eureka model Yang et al., 2020, fixed exponent model fitted with the best five measured isotherms (fixE-5) and free exponent model fitted with the best five measured isotherms (densities calculated by the Eureka model) (freeE-5) for ethylene glycol and propylene glycol

ethylene glycol								
<i>i</i>	1	2	3	4	5	6	7	8
fix Exp.	n_i	1.212	-1.159×10^{-1}	-2.295×10^{-3}	1.680×10^{-2}	-6.420×10^{-3}	3.197×10^{-3}	-5.626×10^{-5}
	t_i	0.0	1.0	4.0	2.5	3.0	-0.5	3.5
	p_i	0.0	-0.5	-2.5	-4.0	-6.0	2.0	2.5
Eureka	n_i	1.074	2.633×10^{-2}	4.291×10^{-2}	-3.898×10^{-3}	2.540×10^{-3}	-1.008×10^{-2}	-2.544×10^{-2}
	t_i	0.0	0.0	-1.0	-1.0	2.0	2.0	2.0
	p_i	0.0	1.0	0.0	-1.0	1.0	-1.0	0.0
fixE-5	n_i	1.212	-1.159×10^{-1}	-2.532×10^{-3}	1.721×10^{-2}	-6.458×10^{-3}	3.291×10^{-3}	-8.070×10^{-5}
	t_i	0.0	1.0	4.0	2.5	3.0	-0.5	3.5
	p_i	0.0	-0.5	-2.5	-4.0	-6.0	2.0	2.5
freeE-5	n_i	1.130	-3.078×10^{-2}	-3.178×10^{-4}	1.007×10^{-2}	-3.721×10^{-3}	2.005×10^{-3}	-4.649×10^{-5}
	t_i	-4.741×10^{-2}	2.164	3.902	3.519	4.460	-3.598×10^{-1}	3.492
	p_i	2.173×10^{-2}	-1.048	-2.492	-4.442	-6.173	2.412	2.476
propylene glycol								
<i>i</i>	1	2	3	4	5	6	7	8
fix Exp.	n_i	1.140×10^1	-1.174×10^{-1}	-2.375×10^{-3}	1.030×10^{-2}	-3.074×10^{-3}	3.834×10^{-3}	-2.591×10^{-5}
	t_i	0.0	1.0	4.0	2.5	3.0	-0.5	3.5
	p_i	0.0	-0.5	-2.5	-4.0	-6.0	2.0	2.5
fixE-5	n_i	1.140	-1.175×10^{-1}	-2.458×10^{-3}	1.104×10^{-2}	-3.480×10^{-3}	3.894×10^{-3}	-1.886×10^{-5}
	t_i	0.0	1.0	4.0	2.5	3.0	-0.5	3.5
	p_i	0.0	-0.5	-2.5	-4.0	-6.0	2.0	2.5
freeE-5	n_i	5.796	-4.775	-1.433×10^{-3}	4.104×10^{-3}	-1.073×10^{-3}	4.485×10^{-3}	5.140×10^{-3}
	t_i	2.859×10^{-1}	3.739×10^{-1}	3.813	2.257	2.783	-6.576×10^{-1}	3.840
	p_i	-2.941×10^{-2}	-4.560×10^{-2}	-2.687	-4.140	-6.082	1.646	3.534×10^{-1}

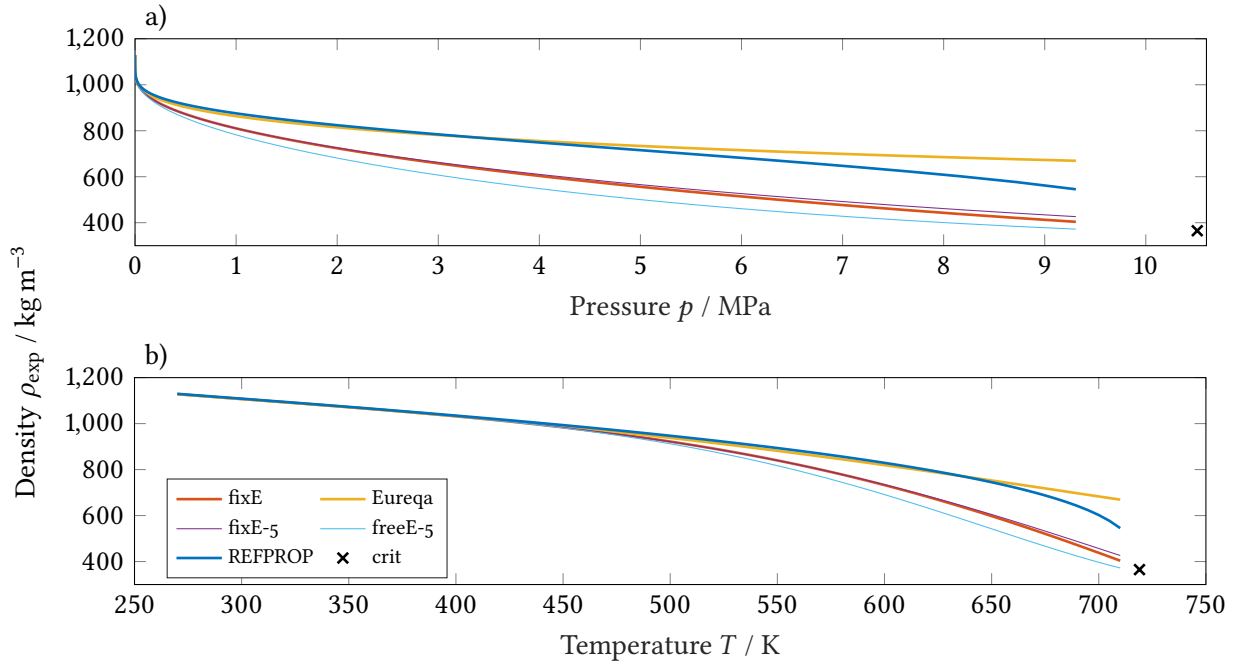


Figure 4.4: Liquid densities at the vapor-liquid saturation line for a) the saturation pressure and b) the saturation temperature obtained from the fundamental equation embedded in Refprop, calculated with the fixed exponent model, the Eureqa model, the fixed exponents model, using the five best measured isotherms, the free exponent model fitted with the best five measured isotherms and the fundamental equation and the critical point embedded in REFPROP [Lemmon et al., 2018](#)

yields the best result with a maximum deviation of -0.20% . We aim to consider boundary conditions, such as the extrapolation behavior, in further investigations.

5 CONCLUSIONS

To decrease the time and even financial expenditure for accurate thermodynamic property modeling, it is necessary to gather suitable experimental data with respect to accuracy and information content. Therefore, we investigated the application of OED to liquid-phase densities of ethylene glycol by calculating the information content of existing experiments along different isotherms. With our resulting model fitted to the most informative five isotherms, we reproduce the measured data with a maximum relative deviation of 0.025% . Compared to the maximum relative deviation of the model involving all eight isotherms of 0.022% , this is a very promising result. These results are validated using the measured data of propylene glycol (0.016% compared to 0.014%). The smaller deviations for propylene glycol can be explained by the model development originally based on these data. By fitting two new models using the best calculated selection of isotherms, we demonstrate that, with OED, sufficiently accurate models can be developed with fewer experiments than traditionally used.

Due to the limitation to already measured data, we are not able to compare these results with a model fitted to the best five freely selected isotherms. At this point, new measurements become necessary in order to compare the models with the best five measured and the best five freely selected isotherms, where we are confident to achieve even better results. Finally, the comparison of the fit with free exponents shows a significant improvement compared to the fixed exponent model, which highlights the importance of model selection, even if this model should not be used outside the measured (p, T)-range. The investigation of the extrapolation behavior underlines this even more, where the use of different thermodynamic criteria beyond the actual measurement data is crucial.

A fortunate circumstance, which should be further investigated, is that the isotherms at ambient temperature are selected last. From an experimental point of view this is advantageous because these are measurements with larger uncertainty since a thermostating task at ambient temperature is often tricky (e. g., a circulating thermostat has to switch between heating and cooling against the ambient temperature).

Our next steps are:

- Measuring the free calculated isotherms, fit the data to the new model and compare the results to the existing models.
- Defining different objective functions in addition to those describing the parameter uncertainty.
- Developing methods to include thermodynamic criteria as boundaries for the model (e. g., extrapolation behavior).
- Using OED based on the nonlinear model (with free exponents) using the sequential process described in [Section 1](#).
- Investigating the influence of the number of terms to deal with the problem of over-fitting.

With these next steps, we aim to create the basis for an OED setup specialized for the measurement of thermodynamic properties. The data for this paper and the calculations performed are provided in the supporting information.

REFERENCES

- Atkinson, A. C.; A. N. Donev; R. D. Tobias (2007). *Optimum Experimental Designs, with SAS*. Vol. 34. Oxford Statistical Science Series. Oxford: Oxford University Press.
- Dechambre, D.; L. W. M. Wolff; C. Pauls; A. Bardow (2014). "Optimal experimental design for the characterization of liquid–liquid equilibria". *Industrial & Engineering Chemistry Research* 53.50, pp. 19620–19627. DOI: [10.1021/ie5035573](#).
- Franceschini, G.; S. Macchietto (2008). "Model-based design of experiments for parameter precision: State of the art". *Chemical Engineering Science* 63.19, pp. 4846–4872. DOI: [10.1016/j.ces.2007.11.034](#).
- Gibson, R. E.; O. H. Loeffler (1939). "Pressure–volume–temperature relations in solutions. I. Observations on the behavior of solutions of benzene and some of its derivatives". *The Journal of Physical Chemistry* 43.2, pp. 207–217. DOI: [10.1021/j150389a003](#).

- Lemmon, E. W.; H. I. Bell; M. L. Huber; M. O. McLinden (2018). *REFPROP - Reference Fluid Thermodynamic and Transport Properties*. Version 10.0. URL: <https://www.nist.gov/srd/refprop>.
- Pázman, A. (1986). *Foundations of Optimum Experimental Design*. Vol. 14. Mathematics and its Applications (East European Series). Translated from the Czech. D. Reidel Publishing Co., Dordrecht.
- Rasch, A.; H. M. Bücker; A. Bardow (2009). "Software supporting optimal experimental design: A case study of binary diffusion using EFCOSS". *Computers & Chemical Engineering* 33.4, pp. 838–849. DOI: [10.1016/j.compchemeng.2008.12.008](https://doi.org/10.1016/j.compchemeng.2008.12.008).
- Sampson, C. C.; X. Yang; J. Xu; M. Richter (2019). "Measurement and correlation of the (p, ρ, T) behavior of liquid propylene glycol at temperatures from (272.7 to 393.0) K and pressures up to 91.4 MPa". *The Journal of Chemical Thermodynamics* 131, pp. 206–218. DOI: [10.1016/j.jct.2018.10.016](https://doi.org/10.1016/j.jct.2018.10.016).
- Schilling, G.; R. Kleinrahm; W. Wagner (2008). "Measurement and correlation of the (p, ρ, T) relation of liquid *n*-heptane, *n*-nonane, 2,4-dichlorotoluene and bromobenzene in the temperature range from (233.15 to 473.15) K at pressures up to 30 MPa for use as density reference liquids". *The Journal of Chemical Thermodynamics* 40.7, pp. 1095–1105. DOI: [10.1016/j.jct.2008.02.020](https://doi.org/10.1016/j.jct.2008.02.020).
- Schmidt, M.; H. Lipson (2009). "Distilling free-form natural laws from experimental data". *Science* 324.5923, pp. 81–85. DOI: [10.1126/science.1165893](https://doi.org/10.1126/science.1165893).
- Schmidt, M.; H. Lipson (2015). *Eureqa*. Version 1.24.0. URL: <http://formulize.nutonian.com/documentation/eureqa/>.
- Setzmann, U.; W. Wagner (1989). "A new method for optimizing the structure of thermodynamic correlation equations". *International Journal of Thermophysics* 10.6, pp. 1103–1126. DOI: [10.1007/bf00500566](https://doi.org/10.1007/bf00500566).
- Sommer, D.; R. Kleinrahm; R. Span; W. Wagner (2011). "Measurement and correlation of the (p, ρ, T) relation of liquid cyclohexane, toluene, and ethanol in the temperature range from 233.15K to 473.15K at pressures up to 30MPa for use as density reference liquids". *The Journal of Chemical Thermodynamics* 43.2, pp. 117–132. DOI: [10.1016/j.jct.2010.08.010](https://doi.org/10.1016/j.jct.2010.08.010).
- Span, R. (2000). *Multiparameter Equations of State*. Springer Berlin Heidelberg. DOI: [10.1007/978-3-662-04092-8](https://doi.org/10.1007/978-3-662-04092-8).
- Thol, M.; I. H. Bell (2020). "Empirical fundamental equations of state for pure fluids and mixtures". *High-Pressure Flows for Propulsion Applications*. American Institute of Aeronautics and Astronautics, Inc., pp. 365–407. DOI: [10.2514/5.9781624105814.0365.0408](https://doi.org/10.2514/5.9781624105814.0365.0408).
- Uciński, D. (2005). *Optimal Measurement Methods for Distributed Parameter System Identification*. Systems and Control Series. Boca Raton, FL: CRC Press.
- Yang, X.; C. C. Sampson; O. Frotscher; M. Richter (2020). "Measurement and correlation of the (p, ρ, T) behaviour of liquid ethylene glycol at temperatures from (283.3 to 393.1) K and pressures up to 100.1 MPa". *The Journal of Chemical Thermodynamics* 144, p. 106054. DOI: [10.1016/j.jct.2020.106054](https://doi.org/10.1016/j.jct.2020.106054).